Development of Low-Exergy-Loss, High-Efficiency Chemical Engines

Investigators

Chris F. Edwards, Associate Professor, Mechanical Engineering; Matthew N. Svrcek, Greg Roberts, Shannon L. Miller, Sankaran Ramakrishnan, Graduate Researchers, Stanford University.

Abstract

In this report we describe our continuing efforts to develop ultra-high efficiency chemical engines. This work is based on what we have termed the 'extreme-states principle'—that reducing efficiency losses due to unrestrained combustion requires performing the reaction at the highest possible internal energy state.

In the exploration of batch processes, we previously completed construction of a free-piston device capable of hosting combustion at volumetric compression ratios in excess of 100:1, with the goal of achieving 60% thermal efficiency. Our work for this past year has included the following: the combustor end-wall seal was redesigned to reduce crevice volume, resulting in significant improvement in cycle efficiency. A peak efficiency of 52% was obtained. The primary focus of this past year and of ongoing work is to understand, design, and optimize the combustion process. To this end an extensive study of Diesel spray behavior at extreme compression ratios was conducted. Spray penetration and dispersion, ignition delay, and liquid phase penetration were all observed and measured using the optical access in the combustor end-wall. A system for measuring gaseous and particulate emissions from the combustion process has also been constructed, and is currently in the initial stages of testing.

Introduction

A majority of energy uses today involve the transformation of chemical bond energy to work, including transportation, power generation, and industrial applications. Improving the efficiency of engines that perform these chemical energy transformations is likely to be a necessary part of any solution to climate change and energy security. Our effort focuses on significantly improving the efficiency of chemical engines by taking a fundamental approach—we start with purely thermodynamic considerations, determine where efficiency losses occur, and attempt to identify and investigate solutions to these losses.

In our first GCEP project, taking this approach led to the identification of an extreme-states principle for combustion engines: The *only* way to reduce the efficiency loss due to unrestrained reaction in an internal combustion engine is to conduct the energy conversion at the highest-possible state of energy density [1]. In this project, we undertake an implementation of the extreme states principle for batch processes (e.g. piston-cylinder engines) by investigating the feasibility of operating at compression ratios of 100:1 or greater. Combustion at such states requires a very different engine design—most likely free-piston with electromagnetic extraction. As a first step, we identified the following key research issues: whether combustion could be successfully conducted (initiated, phased, and completed) under such conditions, and whether the indicated efficiency after real-world-implementation losses would be sufficient to warrant development of such a class of engines.

Development of the above work for a batch process followed the logic path of thermodynamically defining the optimal process, identifying the key parameters for ultra-high efficiency operation, and then implementing and testing in hardware. We are following the same path for the other major class of chemical engines: steady-flow, such as gas turbines. This report details progress made mainly in the batch-flow application; details of our work in steady flow engines will be reported at a future date.

Progress and Results

Demonstration of Low-Irreversibility Combustion by Extreme Compression

The extreme compression device is shown schematically in Figure 1. A free piston is accelerated down the cylinder bore, driven by compressed air from a reservoir via a fast-acting poppet valve. Near the end of its stroke, the piston enters a forged steel combustor section, that contains ports for multiple Diesel fuel injectors and a pressure transducer. A sapphire window is mounted in the end-wall of the combustor, providing full-bore optical access. The cylinder stroke is chosen to be around 2.5 meters to reduce surface-to-volume ratio at the minimum volume (top dead center, or TDC). The combination of high piston speed and high pressure eliminates the possibility of using traditional pressure-energized, oil-lubricated piston seals. Our current strategy uses fixed graphite rings, the diameter of which is within very close tolerance to the cylinder bore—in effect using clearance control between the ring and wall to provide the pressure drop across the piston. Piston position during a run is determined by magnetic sensors distributed along the length of the cylinder, in addition to an optical sensor, similar to an optical encoder, near the combustor section to provide high accuracy piston position measurements near

TDC. Piston position, synchronized with pressure data, provides the indicated work output of the device. Fuel injection is via a high-pressure, common-rail Bosch Diesel pump and injectors, with custom nozzle tips that allow a variety of injection strategies. Our previous GCEP reports provide further detail about the design of the experiment [2, 3].

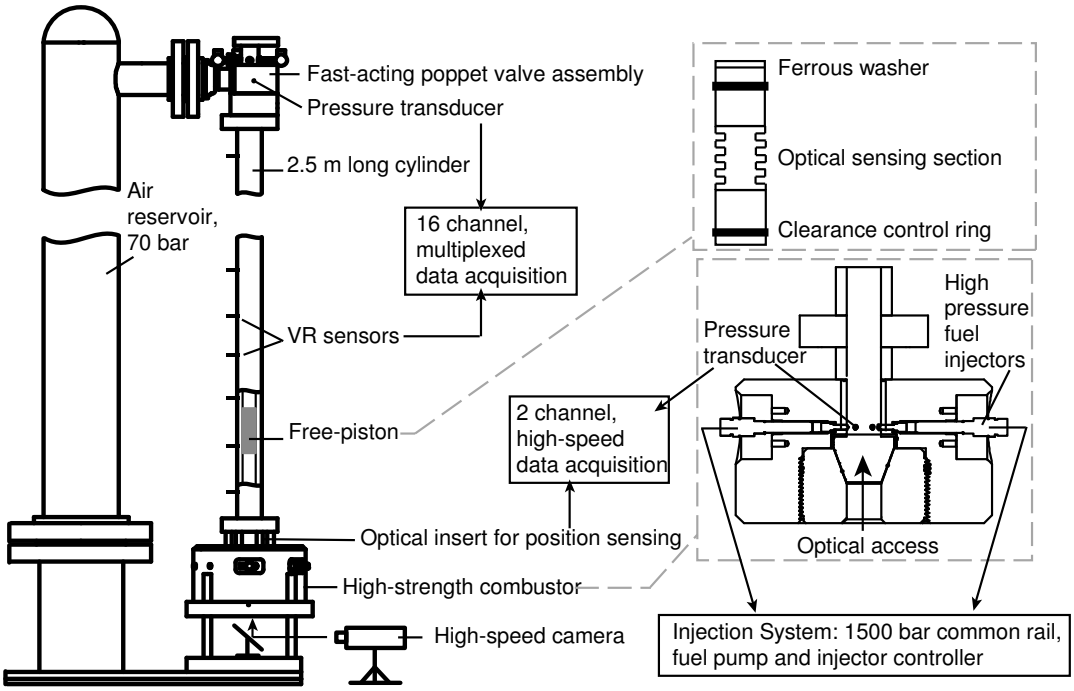

Figure 1: Schematic of the extreme compression device.

Updated Performance Results

In our previous report, we described the intial work-up of the extreme compression device. That initial work focused on doing air-compression only experiments to characterize losses in the device, followed by initial combustion results. Efficiency loss mechanisms for the device can be divided into two general categories: those associated with the compression-expansion process, and those associated with the combustion process. The compression-expansion losses are themselves of two kinds: heat transfer to the chamber walls, and mass loss past the piston (blow-by). The total magnitude of these losses is measured by integrating pressure as a function of volume, thus obtaining the net indicated work of the compression-expansion process during an air-only experiment.

During the past year, the seal around the sapphire window in the combustor end wall was redesigned to eliminate a crevice volume that opens above the window. The original radial seal on the outside edge of the window was replaced with a face seal on the top surface of the window. With the original design, at 100:1 compression ratio roughly 10% of the mass in the combustion section entered the crevice. This crevice gas is cooled to the wall temperature, which, in this single-shot device, remains near room temperature. The fraction of in-cylinder gas entering the crevice increases with increasing compression ratio both because the window is pushed further down by the higher pressure, as well as because the gas density is higher.

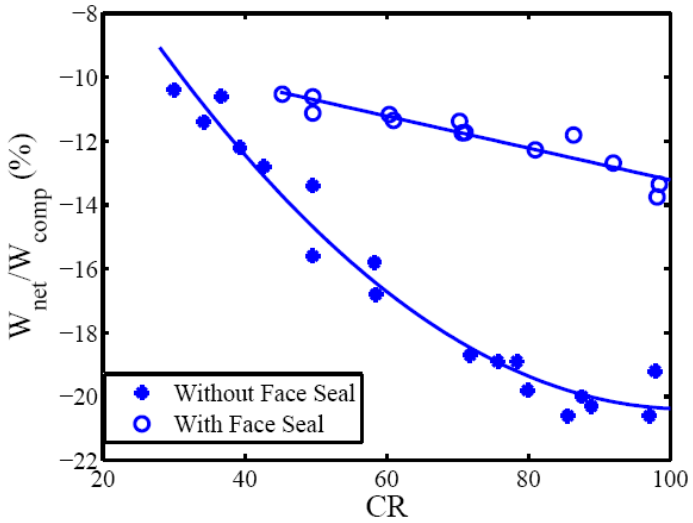

Figure 2: Net work divided by compression work for air-only compression and expansion cycles. Closed circles are for the original combustor seal design, open circles are the new face seal design.

As mentioned above, the total compression-expansion losses are found from the indicated work. One convenient way to express this is as a fraction of the compression work, as shown in Fig. 2 for air-only experiments. The open circles are results with the new seal design—one can clearly see the improvement in net work loss.

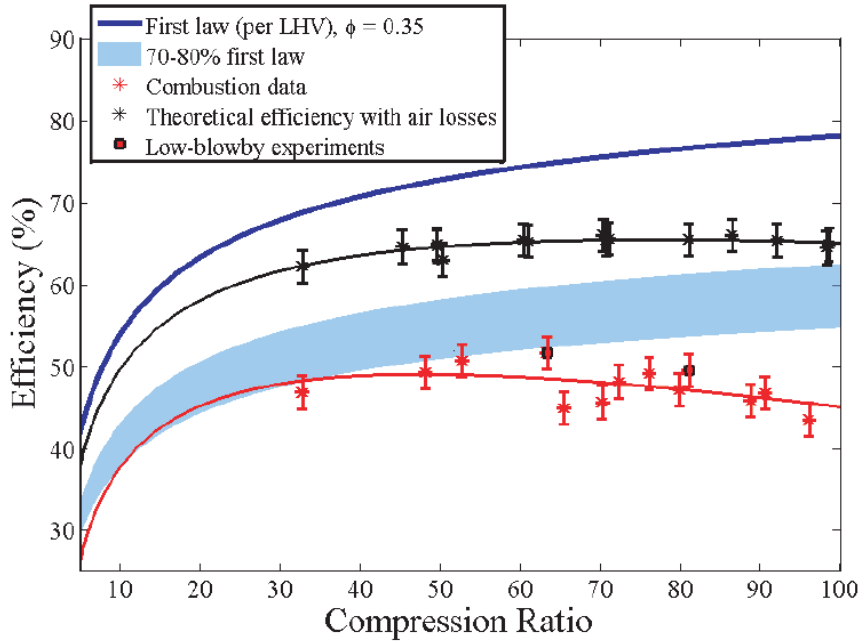

Figure 3: Combusting results (red points), theoretical maximum efficiency (blue line), and theoretical efficiency including compression-expansion losses (black points).

A new set of combustion results were obtained with the new combustor seal design, and are shown in Fig. 3. In these experiments the combustion strategy remains unoptimized, and is identical to the method used in the results reported last year. However, the cycle efficiency is improved at the highest compression ratios due to the reduced crevice losses. A peak efficiency of 52% was achieved at ~60:1 CR. Efficiency rolls off at the higher compression ratios for two general reasons: First, the theoretical efficiency including compression-expansion losses (the black line in Fig. 3) becomes flat at the highest compression ratios due to increased blow-by mass loss. Second, the unoptimized combustion process becomes more lossy as compression ratio increases. One primary reason for this loss is that the compression-expansion process becomes faster near the minimum volume (TDC) as compression ratio increases. The free-piston dynamics are dictated by the pressure forces on the two piston faces—as pressure in the combustion chamber is raised due to higher compression ratio, the acceleration of the piston near TDC also increases. With the current unoptimized combustion strategy, this means that combustion continues well into the expansion stroke, thus reducing efficiency.

Optical Study of Spray and Combustion

Our previous report described the construction of a high-speed schlieren photography system for studying combustion in the extreme compression device, and reported results for non-combustion Diesel spray penetration. In the past year, a study of combusting Diesel sprays was completed, in addition to an investigation of liquid-phase penetration—these results are discussed below.

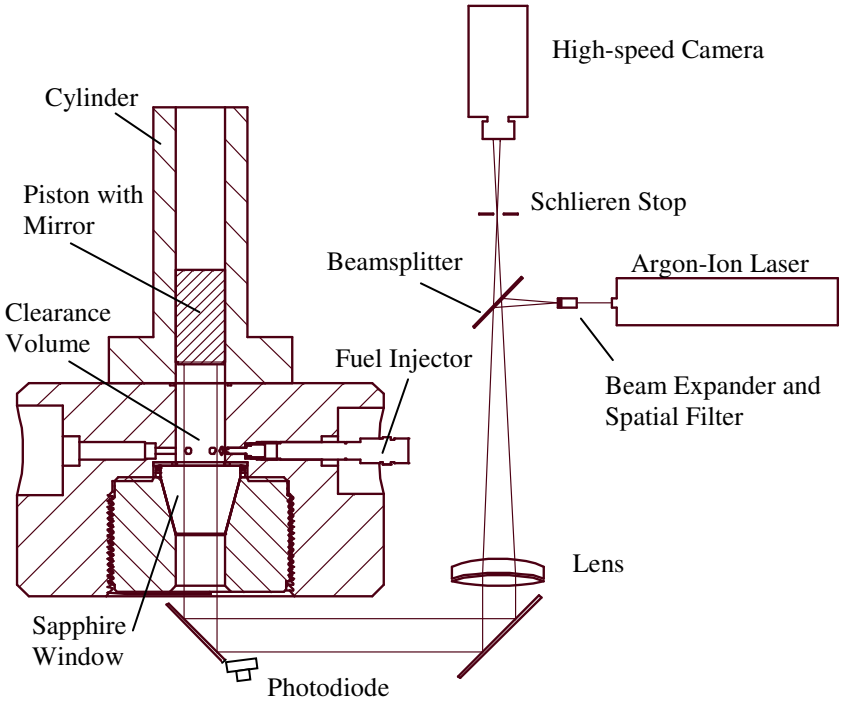

Figure 4: Experimental optics setup.

A schematic of the optical system is shown in Fig. 4. A collimated beam of 488 nm laser light reflects off a mirror mounted on the piston, is focused through an achromatic lens to a schlieren stop and recorded by a high-speed camera. This setup allows simultaneous recording of schlieren effects from gas density variation in the cylinder, extinction in the liquid portion of the spray, and direct luminosity from chemical reaction. In addition, a high-sensitivity photodiode with a UV bandpass filter detects OH chemiluminescence for defining the start of combustion.

CR = 30:1

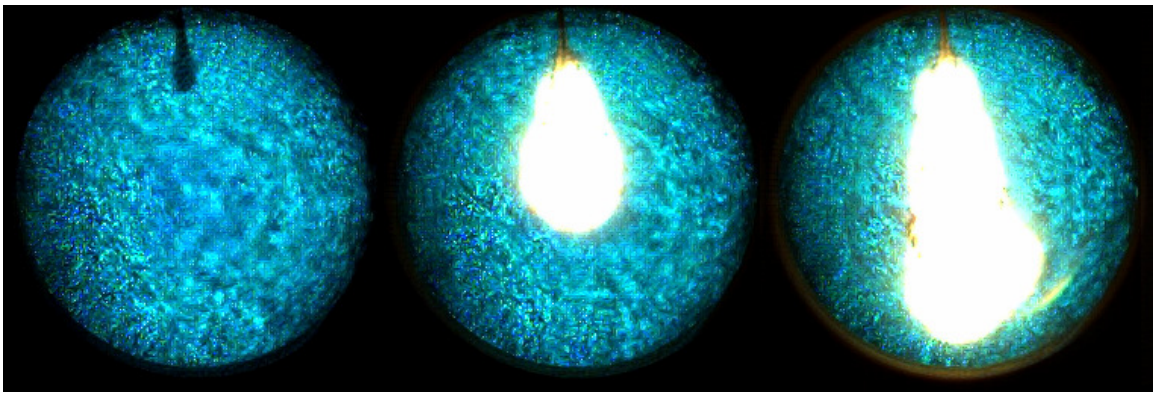

CR = 100:1

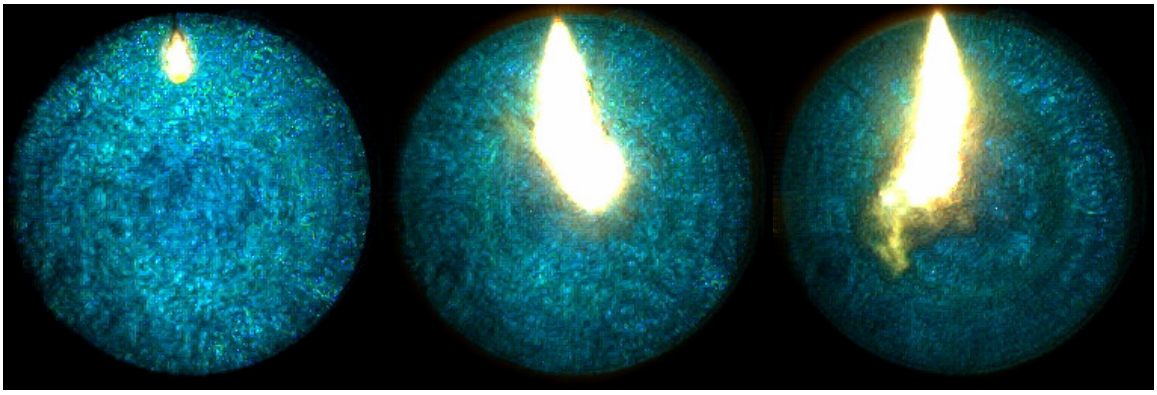

t = 0.11 ms ASOI 0.5 ms 1.0 ms

Figure 5: Diesel spray images for 30 and 100:1 compression ratios, taken 0.11, 0.5, and 1.0 ms after start of injection.

Figure 5 shows a sequence of images from the combusting spray experiments, for 30:1 and 100:1 compression ratio. Several qualitative observations can be made from the images. For example, the first image in each sequence shows that the ignition delay is in general much shorter for the 100:1 compression ratio. The lift-off length (distance from the injector tip to the reaction front) is also shorter. The most striking difference, however, is the behavior of the spray penetration, especially during the latter portion of the spray event. In the 30:1 CR case, the spray proceeds across the chamber as expected, and looks very much like Diesel sprays in conventional engine conditions, widely reported in Diesel spray literature. However, for the 100:1 CR case, the spray is seen to

not penetrate as far into the chamber, and is significantly affected by in-cylinder gas motion. There also appears to be some extinction of the soot luminosity in the spray tip region.

As was previously done for the non-reacting spray study, quantitative spray penetration results are obtained by processing the camera images to define the spray region. In the combusting case, the spray region is the combination of the dark region near the injector tip from light extinction in the liquid phase, the luminous soot combustion region, and the dark region near the edges of the spray resulting from schlieren effects in the fuel vapor and combusted gases. The resulting spray penetration (distance from injector tip to furthest extent of spray region) is shown as a function of time in Fig. 6 below.

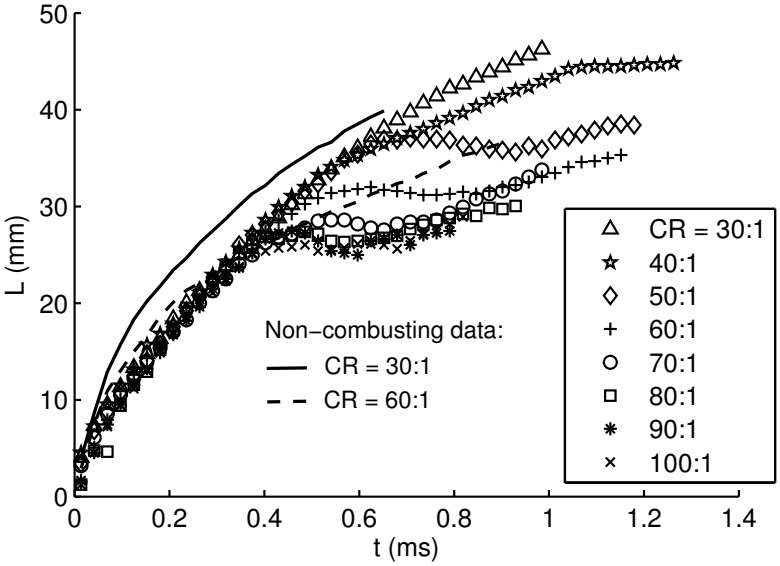

Figure 6. Combusting spray penetration vs. time. Data from the non-combusting results for 30 and 60:1 CR are shown for comparison.

One particularly notable feature in the data is that for the highest compression ratios, the spray appears to stop penetrating and even retreat somewhat during the middle portion of the spray event, around 0.6 ms after start of injection. This is a result of the interaction of the spray with in-cylinder fluid motion, as seen qualitatively in the image sequences. More specifically, the fluid motion is believed to be a strong axial jet flowing from the piston face towards the end-wall of the combustor. This jet is formed in a manner similar to the 'rolling vortex' phenomenon commonly seen in piston engines. As the piston travels down the cylinder, boundary layer gas is scraped towards the center of the cylinder by the piston and forced down the axis. This phenomenon is unusually strong in the extreme compression device due to the very long stroke and high piston speed. In addition to observations made with the schlieren system for air-only experiments, fluid modeling of the compression stroke in Fluent shows the formation of this axial jet and appears to confirm this hypothesis.

A further important observation is that the jet-spray interaction only becomes apparent above ~60:1 CR, and becomes stronger as compression ratio increases. This is

because the ratio of the fuel density to the ambient gas density becomes low (~8:1 for 100:1 compression ratio). As a result momentum transfer between the ambient gas and the spray jet is strong, and in-cylinder fluid mechanics become important in understanding the spray behavior. Finally, it must be noted that the absence of the jet interaction in the non-combusting results is likely due to the change in the window seal design discussed in the previous section, not an effect of the presence or absence of reaction. The original seal design resulted in a gas 'sink' that changed the interaction of the axial jet with the spray in the older non-combusting results.

Ignition delay was also quantitatively measured via detection of combustion luminosity on a photodiode. Ignition delay was defined as the time from the first apperance of the spray jet in the camera images, to the time at which the luminosity signal on the photodiode rose to 10 standard deviations above the background noise. This definition is somewhat arbitrary, but is repeatable from one experiment to the next, allowing study of ignition delay trends. The results are shown in Fig. 7. .

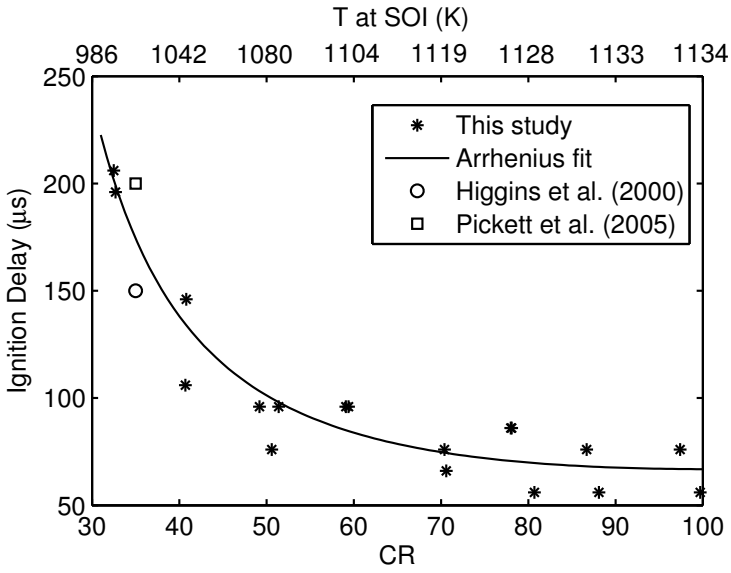

Figure 7. Ignition delay vs. compression ratio, shown with an Arrhenius fit as described in the text. For comparison, data from two other ignition delay studies are shown [4, 5]. Temperature at start of injection is shown on the top axis.

Diesel spray ignition delay is often fit to an Arrhenius relationship of the form

$$\tau = A\left(\frac{\rho_a}{\rho_0}\right)^{-n} \exp\left(\frac{E}{RT_a}\right)$$

where ρ_a and T_a are the ambient gas density and temperature. The log of ignition delay is usually plotted against $1/T_a$ for various ambient density conditions; linearity of the data for each density indicates a good fit to Arrhenius form. This method is complicated here by the fact that density and temperature are not independent. A fit to the Arrhenius form

above is attempted by using a value of $n = 1.3$ for the density exponent found empirically by Pickett et al. and others [5]. The ambient gas density and temperature are calculated assuming isentropic compression of the core gas from initial conditions to the experimentally measured pressure. The resulting fit is plotted in Fig. 7 and agrees reasonably well with the data. This indicates that the ignition delay continues to follow an Arrhenius relation with respect to the temperature at start of injection, even up to the high compression ratios.

A study of the penetration of the liquid-phase region of the spray jet was also carried out. In order to visualize the liquid region, the optical setup was changed to provide diffuse back-illumination of the spray. The liquid region appears as a dark area in the image as shown in Fig. 8, as a result of scattering and absorption by the liquid droplets. The liquid length is defined as the distance from the injector tip to the furthest extent of the liquid region. Liquid length experiments were performed with pure nitrogen in the cylinder to produce a non-reacting spray.

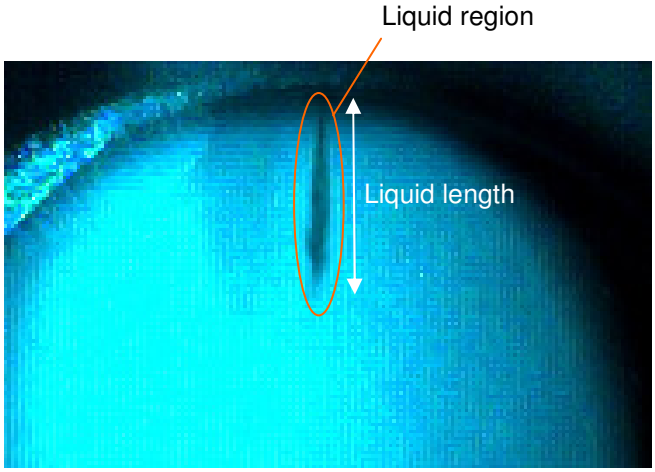

Figure 8. Image from liquid length experiment for 30:1 CR, 0.27 ms after SOI.

The liquid region is expected to penetrate rapidly, and then reach a steady-state length at the point where vaporization occurs. This behavior is seen in the liquid length vs. time data shown in Fig. 9 . However, as a result of the changing conditions during injection (i.e. the piston is moving towards TDC and then away), the steady-state liquid length decreases as TDC is approached, reaches a minimum value, and then increases again. The turbulent nature of the liquid region tip can also be seen in the rapid fluctuations in liquid length seen in Fig. 9. The liquid length value at TDC is plotted for several compression ratios in Fig. 10. One can see that the liquid length generally decreases with increasing compression ratio, but appears to approach an asymptote of ~ 4 mm as compression ratio reaches ~80:1. In general, 4 mm is a very short liquid length, due to the very high compression ratio, which indicates that impingment of the liquid core on cylinder walls or the piston face is unlikely to be a concern.

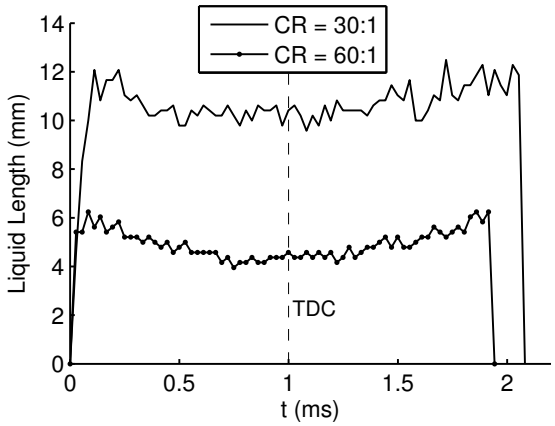

Figure 9. Liquid length vs. time.

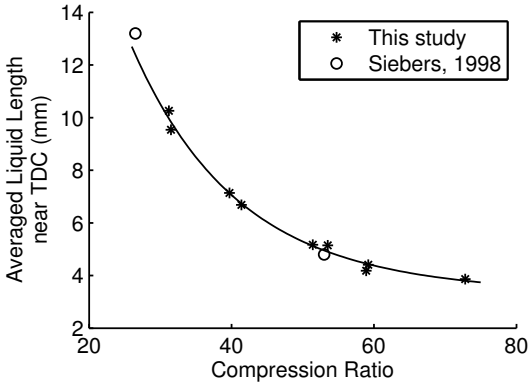

Figure 10. Average liquid length at TDC, vs. CR. The exponential fit (solid line) is to the data from this study (circles). Data from Siebers shown for comparison [6].

Current and Future Work – Emissions Analysis

A system for the analysis of emissions from combustion in the extreme compression device is currently being constructed and tested. This will play a critical role in continued design and testing of the combustion strategy. The system consists of two parts: one for measuring NO, CO, CO_2, O_2, and total hydrocarbons, and one for measuring particulate matter.

Because the extreme compression device is single-shot, the walls remain near room temperature during the course of an experiment. As a result the water produced from combustion will condense onto the cylinder walls immediately after an experiment. This presents a problem in measuring emissions, in particular for hydrocarbon emissions measurements with water-miscible fuels such as alcohols. To prevent water condensation, a heating system for the cylinder and combustor has been designed and implemented. Electric-resistance band heaters have been placed along the cylinder and around the combustor base section. Foam insulation was installed around the entire system. Thermocouples and PID temperature controllers allow maintenance of a temperature set point. The system can operate at a maximum temperature of 125 °C, but is currently operated at 80 °C, which is well above the dew-point for the water fraction obtained in combustion.

Following a combustion experiment, the piston comes to rest somewhere in the middle of the cylinder. An exhaust valve in the combustor is then opened and the combustion products exit the cylinder, at which point they are divided into two streams. One stream remains 'wet' and is passed through a heated line and into a flame-ionization detector, which measures the total hydrocarbon content. The remaining gas passes through an ice-bath, causing the water and soluble fuel species to condense out. The dry gas is stored in a Tedlar sample bag, which is then connected to a Horiba suite of gas analyzers. The sample gas is simultaneously passed through NDIR analyzers for CO and CO_2, a magneto-pneumatic analyzer for O_2, and a chemiluminescence analyzer for NO. The analog output of all five analyzers (including the FID) is read by a data acquisition

board. The sample size from a single experiment is large enough that all of the analyzers reach a steady-state value before the sample gas is depleted.

In general, particulate can be measured in-situ or ex-situ. Ex-situ techniques—passing the gas out of the engine and into an external analyzer—depend on a steady-state condition being reached in the engine and measurement apparatus. In a single-shot device such as this, in which a steady-state condition is not reached, thermophoretic deposition of particulates on the cylinder and tubing walls can significantly impact the measurement. For this reason we chose an in-situ technique—absorption of a laser beam by the particulates within the combustion chamber. A helium-neon laser beam at 632.8 nm wavelength is introduced via an optical fiber. The beam is collimated before passing through a small sapphire window in one of the fuel injector ports in the combustor. The beam passes across the combustor bore, where it enters a second sapphire window in the diametrically opposed port, is collected in a second optical fiber, and then passes onto a photodetector. The fractional reduction in the detected beam amplitude is a function of the particulate volume fraction in the beam path.

Preliminary tests of the emissions system have been conducted. The next step in the research will be to begin systematically exploring the emissions performance of the extreme compression device as a function of compression ratio and equivalence ratio.

Publications

1. Miller, S.L., *Theory and Implementation of Low-Irreversibility Chemical Engines*. Ph.D. dissertation, Dept. of Mech. Eng., Stanford Univ., Stanford, CA, 2009.
2. Svrcek, M.N., Miller, S.L., and Edwards, C. F., Diesel Spray Behavior at Compression Ratios up to 100:1. Submitted to *Atomization and Sprays*. (2010).

References

1. Teh, K.-Y., Thermodynamics of Efficient, Simple-Cycle Combustion Engines..
2. C. F. Edwards, S. L. Miller, M. N. Svrcek, and S. Ramakrishnan, Development of Low Exergy Loss, High Efficiency Chemical Engines, GCEP Annual Technical Report, June, 2008
3. C. F. Edwards, S. L. Miller, M. N. Svrcek, and S. Ramakrishnan, Development of Low Exergy Loss, High Efficiency Chemical Engines, GCEP Annual Technical Report, June, 2009
4. Higgins, B., Siebers, D., and Aradi, A., Diesel-Spray Ignition and Premixed-Burn Behavior, SAE Paper 2000-01-0940.
5. Pickett, L., Siebers, D., and Idicheria, C., Relationship Between Ignition Processes and the Lift-Off Length of Diesel Fuel Jets, SAE Paper 2005-01-3843.
6. Siebers, D., Liquid-Phase Fuel Penetration in Diesel Sprays, SAE Paper 980809.

Contacts

Christopher F. Edwards: cfe@stanford.edu
Matthew Svrcek: msvrcek@stanford.edu
Greg Roberts: gregrob@stanford.edu
Sankaran Ramakrishnan: rsankar@stanford.edu